Title	The function of p120 Catenin in Filopodial Growth and Synaptic Vesicle Clustering in Neurons
Author(s)	Chen, C; Li, P; Madhavan, R; Peng, HB
Citation	Molecular Biology of Cell, 2012, v. 23 n. 14, p. 2680-2691
Issued Date	2012
URL	http://hdl.handle.net/10722/152727
Rights	Molecular Biology of the Cell. Copyright © American Society for Cell Biology

The function of p120 catenin in filopodial growth and synaptic vesicle clustering in neurons

Cheng Chen*,†, Pan P. Li†, Raghavan Madhavan, and H. Benjamin Peng
Division of Life Science, State Key Laboratory of Molecular Neuroscience, Hong Kong University of Science and Technology, Clear Water Bay, Hong Kong, China

ABSTRACT At the developing neuromuscular junction (NMJ), physical contact between motor axons and muscle cells initiates presynaptic and postsynaptic differentiation. Using *Xenopus* nerve–muscle cocultures, we previously showed that innervating axons induced muscle filopodia (myopodia), which facilitated interactions between the synaptic partners and promoted NMJ formation. The myopodia were generated by nerve-released signals through muscle p120 catenin (p120ctn), a protein of the cadherin complex that modulates the activity of Rho GTPases. Because axons also extend filopodia that mediate early nerve–muscle interactions, here we test p120ctn's function in the assembly of these presynaptic processes. Overexpression of wild-type p120ctn in *Xenopus* spinal neurons leads to an increase in filopodial growth and synaptic vesicle (SV) clustering along axons, whereas the development of these specializations is inhibited following the expression of a p120ctn mutant lacking sequences important for regulating Rho GTPases. The p120ctn mutant also inhibits the induction of axonal filopodia and SV clusters by basic fibroblast growth factor, a muscle-derived molecule that triggers presynaptic differentiation. Of importance, introduction of the p120ctn mutant into neurons hinders NMJ formation, which is observed as a reduction in the accumulation of acetylcholine receptors at innervation sites in muscle. Our results suggest that p120ctn signaling in motor neurons promotes nerve–muscle interaction and NMJ assembly.

INTRODUCTION

During the development of the vertebrate neuromuscular junction (NMJ), initial contact between nerve and muscle facilitates signaling between the synaptic partners. This bidirectional signaling leads to the aggregation of acetylcholine receptors (AChRs) in the postsynaptic membrane of muscle to a density of ~10,000/μm^2 (Fertuck and Salpeter, 1976) and to the accumulation of synaptic vesicles (SVs) and mitochondria within the nerve terminal (Hughes *et al.*, 2006; Lee and Peng, 2006, 2008). In molecular terms, the best-understood

part of this early neuromuscular signaling involves the activation of the muscle-specific tyrosine kinase by the nerve-derived factor agrin (Glass *et al.*, 1996), which results in the clustering of AChRs by the protein rapsyn in an actin polymerization–dependent manner (Glass and Yancopoulos, 1997; Banks *et al.*, 2003; Madhavan and Peng, 2005). On the presynaptic side, after nerve contact with muscle, active zones appear and SVs become concentrated in the incipient nerve terminals (Weldon and Cohen, 1979; Nakajima *et al.*, 1980; Buchanan *et al.*, 1989), but the control of presynaptic differentiation remains poorly described. Although previous work suggested that several fibroblast growth factors (FGFs), neurotrophins, and cell adhesion molecules expressed by muscle influence the transformation of motor axon growth cones into nerve terminals specialized for neurotransmitter release (Dai and Peng, 1995; Fitzsimonds and Poo, 1998; Fox and Umemori, 2006; Fox *et al.*, 2007; Johnson-Venkatesh and Umemori, 2010), further studies are needed to understand the mechanistic underpinnings of presynaptic development at the NMJ.

When growing motor axons reach muscle, synaptic differentiation is induced locally in nerve and muscle at the sites where they contact each other, which suggests that physical interaction between the synaptic partners facilitates NMJ assembly. Although the

role of growth cones in guiding elongating axons over long distances to their targets has been extensively studied (Lin and Forscher, 1993; Dent *et al.*, 2003), the regulation of short-range contacts between nerve and muscle is poorly understood. Over the past decade, however, several groups have shown that muscle cells extend filopodial processes (termed myopodia) that interact with nerve and promote NMJ formation (Uhm *et al.*, 2001; Ritzenthaler and Chiba, 2003; Madhavan *et al.*, 2006). Myopodia are induced in vertebrate muscle by agrin, and we have shown that this involves signaling in muscle by the protein p120 catenin (p120ctn; Uhm *et al.*, 2001; Madhavan *et al.*, 2006).

A component of the cadherin cell adhesion complex, p120ctn was first identified as a Src tyrosine kinase substrate whose phosphorylation correlates with cell transformation (Reynolds *et al.*, 1989). The p120ctn protein, which is widely expressed, controls processes related to cell adhesion, motility, and morphogenesis, and p120ctn is a critical regulator of cadherin stability, as well as of the activity of Rho-family GTPases (Reynolds, 2007). Overexpression of p120ctn in fibroblasts generates "dendritic processes" and enhances cell motility, and this is generally believed to depend on the positive and negative influences of p120ctn on the actions of Rac/Cdc42 and Rho GTPases, respectively (Reynolds *et al.*, 1996; Anastasiadis and Reynolds, 2001). Our previous work showed that interfering with p120ctn's ability to signal normally through Rho GTPases hindered agrin-dependent myopodial assembly and NMJ establishment (Madhavan *et al.*, 2006). It is intriguing that p120ctn also differentially regulates Rac and Rho GTPases in central neurons, and p120ctn deletion in these neurons suppresses the formation of dendritic spines (Elia *et al.*, 2006); dendritic spines are postsynaptic protrusions in central neurons where excitatory synapses are often found (Harris and Kater, 1994; Hotulainen *et al.*, 2009). Several studies now support the view that p120ctn and its close relative δ-catenin promote synaptogenesis in the CNS (Arikkath and Reichardt, 2008; Brigidi and Bamji, 2011).

At the developing NMJ, nerve–muscle contact is mediated not only by myopodia, but also by axonal filopodia. A recent study from our group showed that muscle cells elicit the growth of filopodia in the motor axons that approach them, and further that basic FGF (bFGF) is a factor associated with the muscle surface that induces filopodia in axons (Li *et al.*, 2011). In that study we also presented the first evidence suggesting that nerve–muscle interactions mediated by neuronal filopodia facilitate NMJ development. Because p120ctn is expressed in neural and nonneural tissues and induces filopodial processes in many types of cells, we investigate here the potential involvement of p120ctn in filopodial formation in axons during NMJ establishment. We carried out molecular, cell-biological, and biochemical experiments using *Xenopus* nerve and muscle primary cultures and mammalian cell lines and present results that suggest that p120ctn signaling in neurons generates axonal filopodia, promotes SV clustering, and facilitates NMJ development.

RESULTS

Filopodia in *Xenopus* spinal neurons

Filopodia are motile cellular processes that promote cell–cell interaction. At the developing NMJ, filopodia are extended by both neurons and muscle cells during the establishment of contacts between these synaptic partners. Previous work has shown that cultured neurons extrude slender filopodial processes in an actin polymerization–dependent manner (Gallo and Letourneau, 2004). We observed that in primary cultures of *Xenopus* spinal neurons, filopodia developed at growth cones and along the length of elongating axons and often extended out preferentially at varicosities, which

are sites enriched in molecules and organelles found in the presynaptic apparatus of nerve terminals (Hughes *et al.*, 2006; Siksou *et al.*, 2011). As we recently reported (Li *et al.*, 2011), filopodia appeared in roughly equal numbers on both sides of axons when cultured alone, but in nerve–muscle cocultures more filopodia developed on the muscle-facing side of axons. Moreover, where axonal filopodia contacted muscle they induced AChR clustering, indicating NMJ development. This is illustrated by the example in Figure 1, A and B.

Involvement of p120ctn in filopodial formation and SV clustering in spinal neurons

Signaling by p120ctn generates motile processes in many cell types, including muscle cells (Madhavan *et al.*, 2006), but whether p120ctn works similarly in spinal neurons was not previously examined. Consistent with the known widespread expression of p120ctn in neural and nonneural tissues, p120ctn was detected in cultured *Xenopus* spinal neurons by immunolabeling: an anti-p120ctn antibody stained entire neurons (Figure 1, C–E) but control antibodies did not (Figure 1, F–H). Here synapsin-I immunolabeling was also performed to localize SVs, and, in accord with previous studies (Dai and Peng, 1996; Lee and Peng, 2006, 2008), distinct puncta of SVs were observed along the axons of spinal neurons, frequently in association with varicosities where filopodia often emanated (Figure 1, E and H). In contrast to the punctate localization of SVs, p120ctn was distributed diffusely along the axon.

To test whether p120ctn plays a role in the formation of filopodia in *Xenopus* spinal neurons, we manipulated p120ctn signaling using molecular methods. Because knocking down p120ctn in *Xenopus* hinders embryonic development (Paulson *et al.*, 1999; Ciesiolka *et al.*, 2004; Fang *et al.*, 2004), we adopted an overexpression strategy using wild-type and mutant forms of p120ctn (Madhavan *et al.*, 2006). Pure nerve cultures were prepared from *Xenopus* embryos injected with mRNAs encoding wild-type p120ctn (WTp120) tagged with green fluorescent protein (GFP), GFP alone (as control), or a GFP-tagged p120ctn deletion mutant (Δp120) that lacks sequences important for regulating Rho GTPases (Anastasiadis *et al.*, 2000). Neurons expressing the exogenous proteins were identified by green fluorescence, and the effects of these proteins on filopodial formation in live axons were examined 18 h after seeding the neurons. Nearly twice as many filopodia were detected in neurons expressing WTp120 (Figure 2, D and E) compared with those expressing GFP alone (Figure 2, A and B), but in neurons expressing Δp120 (Figure 2, G and H) filopodial formation was greatly reduced compared with control. These results were quantified in terms of filopodial densities by counting filopodia in many axon segments chosen randomly from multiple cultures and calculating the number of filopodia per unit length of axon (Figure 2J). Here we also conducted time-lapse recordings to follow the formation of filopodia so as to address how p120ctn might generate filopodia. As quantified in Figure 2K, the rate of new filopodial assembly in WTp120-expressing neurons was twice that calculated in control, whereas in Δp120-expressing neurons filopodia were rarely extended during the recording periods. These results suggest that p120ctn signaling promoted filopodial extension in spinal neurons.

Axonal filopodia were often associated with varicosities that are enriched in SVs (Figure 1, A and B; Li *et al.*, 2011). We therefore examined whether the effect of p120ctn on filopodial formation in neurons was also accompanied by changes in SV clustering. Because these experiments involved the observation of live axons, SV clusters were identified by the uptake of FM4-64, a lipophilic styryl dye that fluoresces red. SVs take up this dye when they fuse with the neuronal membrane and recycle due to experimentally induced
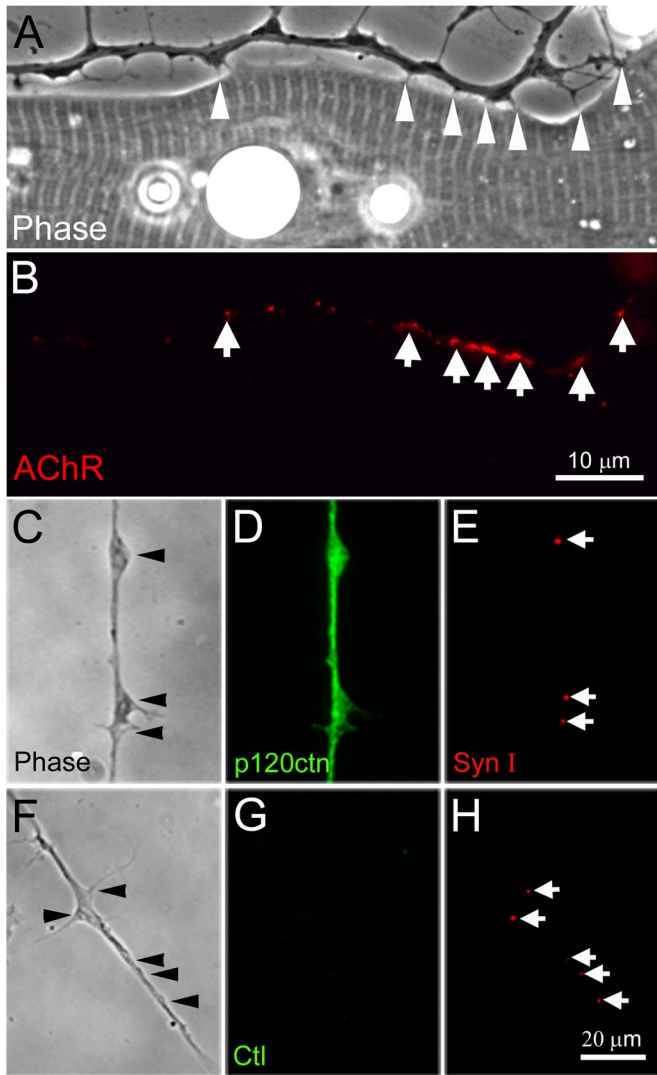
FIGURE 1: Filopodia and SV clusters in *Xenopus* spinal neurons. (A, B) Axonal filopodia contacted muscle cells in cocultures (arrowheads in A) and R-BTX labeling showed that AChR clusters formed at these contacts (arrows in B). (C–E) Eighteen-hour-old spinal neurons were fixed and coimmunolabeled with anti-p120ctn and anti–synapsin-I antibodies. A diffuse distribution of p120ctn was observed in axons with no specific concentration at SV puncta. (F–H) No signal was detected if the primary antibody was replaced with anti–hemagglutinin tag antibody (G). SV clusters labeled by anti–synapsin-I antibody often existed at the base of filopodia or at varicosities (C, E and F, H).

depolarization by high-potassium medium (Dai and Peng, 1996), and thus this labeling procedure can mark functional SV pools within the axon. Our previous study showed that SV puncta marked by the FM dye in live neurons were correspondingly labeled by SV antibodies after fixation (Dai and Peng, 1996). Here FM4-64–labeled SV clusters were once again observed within axons in live cultures (Figure 2, C, F, and I), and overexpression of wild-type p120ctn increased the density of these SV clusters compared with the expression of GFP (Figure 2, C and F). On the other hand, introduction of the Δp120 mutant in neurons decreased SV clustering (Figure 2I). Quantification of data from three separate cultures demonstrated that the number of SV clusters/unit length of axon was doubled in WTp120 neurons and more than halved in Δp120 neurons compared with

GFP-expressing control neurons (Figure 2J). These results suggest that p120ctn signaling promoted, in addition to filopodial formation, SV aggregation in spinal neurons.

The role of p120ctn/Rho signaling in filopodial and SV cluster formation

To further monitor the cellular changes induced by exogenous p120ctn, we examined fixed neurons. Labeling with anti–synapsin-I antibody showed, in agreement with the foregoing results, that neurons overexpressing WTp120 had more SV puncta than did GFP-neurons, whereas Δp120-expressing neurons exhibited a scarcity in SV puncta (Figure 3, A–F). We also sought to visualize the distribution of F-actin in these neurons because processes such as filopodia are generated by the actions of proteins (like p120ctn) that control actin dynamics. Labeling with fluorescent phalloidin showed that F-actin was localized throughout axons and enriched in filopodia in GFP-neurons (Figure 3, G and H), and the overexpression of WTp120 led to a more dramatic display of filopodial F-actin labeling (Figure 3, I and J); expression of Δp120, in contrast, caused a paucity in labeling except along the axon shaft (Figure 3, K and L).

A large variety of cellular proteins regulate F-actin assembly and disassembly, and among these the Rho-family GTPases are well known for their indispensable function in controlling actin dynamics (Mackay *et al.*, 1995). The modulation Rho GTPase activity by p120ctn is involved in the formation of filopodia and stress fibers (Nobes and Hall, 1995; Anastasiadis *et al.*, 2000), and the p120ctn deletion mutant (Δp120) used here (whose expression lowered filopodial density in axons) poorly inhibits RhoA compared with wild-type p120ctn (Anastasiadis *et al.*, 2000). This suggested a potential function of RhoA in mediating p120ctn-dependent filopodial assembly in spinal neurons, and to test this directly, we treated neurons with a cell-permeant form of C3 transferase, a specific inhibitor of RhoA (Aktories and Just, 2005). In GFP-neurons, application of C3 toxin (1 μg/ml, 1 h) increased the number of axonal filopodia (Figure 4, A and A′) and also enhanced the density of SV puncta along axons (Figure 4, C and C′). In WTp120-neurons (Figure 4, D–F), however, this treatment did not elevate the density of either filopodia or SV puncta (Figure 4, D′–F′), suggesting that the overexpression of WTp120 by itself had maximally suppressed RhoA. Most noticeably, in Δp120-expressing neurons, which had few filopodia or SV puncta (Figure 4, G–I), C3 toxin boosted the assembly of both structures significantly (Figure 4, G′–I′). The results are quantified using data from multiple experiments in Figure 4, J and K.

RhoA activates the Rho-associated protein kinase-1 (ROCK-1) to block the extension of actin-rich processes such as filopodia (Olivo *et al.*, 2000). Thus the suppression of filopodial assembly in Δp120-expressing neurons could have resulted from poor inhibition of RhoA and overactivation of ROCK-1. To test this premise, we examined whether filopodial formation was influenced by the specific ROCK inhibitor Y27632, which competes with ATP for binding to the kinase's catalytic site (Ishizaki *et al.*, 2000). Neurons expressing GFP, WTp120ctn, and Δp120 were treated without or with Y27632 for 1 h (unpublished data) or 6 h (Figure 5, A–I′). In GFP-neurons addition of Y27632 generated more filopodia than was normal (Figure 5, A and A′), as might be expected from the inhibition of ROCK; of note, SV puncta were also increased after drug treatment (Figure 5, C and C′). In contrast, Y27632 treatment enhanced neither filopodial assembly nor SV clustering in WTp120 neurons (Figure 4, D–F and D′–F′), consistent with the results obtained with C3 toxin treatment. Of importance, in Δp120-expressing neurons, the densities of filopodia and SV clusters increased significantly after exposure to Y27632 (Figure 5, G′–I′). The quantification of results using data pooled from
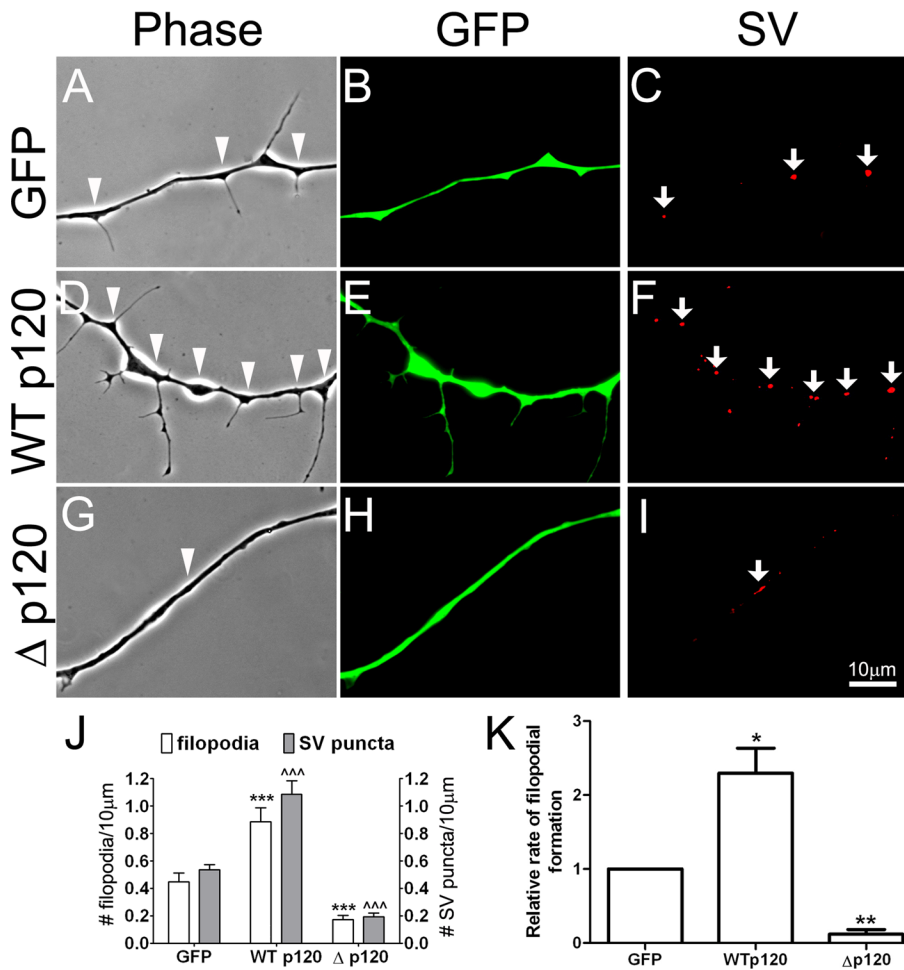
FIGURE 2: The involvement of p120ctn in the formation of axonal filopodia and SV clusters. (A–C) Control axons expressing GFP exhibited filopodia and SV clusters (arrows in C) along their length. (D–F) Overexpression of GFP-linked, wild-type p120ctn (WTp120) in neurons enhanced axonal filopodial formation (arrowheads in D) and SV clustering (arrows in F). (G–I) Expression of mutant p120ctn with a deletion of the Rho-regulatory domain (Δp120, also linked with GFP) suppressed filopodial and SV cluster formation along the axon. (J) Quantification based on data collected from cultures prepared from three separate batches of mRNA-injected embryos. The densities of filopodia (left y-axis) and SV puncta (right y-axis) per 10 μm of axonal length were calculated. (K) To examine filopodial dynamics in neurons expressing exogenous proteins, time-lapse recording was carried out. Neurons were imaged for 10 min at 1-min time intervals. and the rates of new filopodial growth were calculated for GFP-, WTp120-, and Δp120-expressing neurons; these values were normalized relative to that in GFP-expressing neurons. WTp120-expressing neurons showed a twofold increase in the rate of filopodial assembly compared with GFP-neurons, whereas in Δp120-expressing neurons the rate of filopodial formation was very low. Data are shown as mean and SEM. *$p < 0.05$, **$p < 0.01$, and ***,^^^$p < 0.001$ compared with control.

recently we found that bFGF is expressed on the surface of *Xenopus* embryonic muscle cells and that bFGF signaling through FGF receptor 1 (FGFR1) in spinal neurons plays a role in the preferential extension of filopodia by axons toward nearby muscle cells (Li *et al.*, 2011). However, the signals generated by bFGF/FGFR1 in neurons that induce axonal filopodia are unknown. Because p120ctn functions downstream from many growth factor receptors to effect morphological changes in cells (Reynolds, 2007) and because p120ctn enhanced the assembly of axonal filopodia (see earlier discussion), it was of interest to test whether this molecule also mediated bFGF-dependent filopodial growth in spinal neurons.

Addition of purified bFGF increased the density of filopodia in wild-type *Xenopus* spinal neurons (Li *et al.*, 2011). Here spinal neurons expressing GFP, WTp120ctn, or Δp120 were exposed to control or bFGF-added medium for 6 h and then examined live. Treatment with bFGF enhanced the formation of filopodia in GFP-neurons (Figure 6, A and B, vs. A′ and B′), as seen previously using neurons expressing no exogenous proteins (Li *et al.*, 2011), and bFGF also increased the number of SV puncta in these neurons (Figure 6, C and C′). Neurons expressing WTp120 (Figure 6, D–F) had a higher-than-normal density of filopodia and SV clusters (as before), and this density was close to that attained in GFP-neurons after exposure to bFGF; addition of bFGF very slightly increased filopodial assembly but not SV clustering in WTp120-neurons (Figure 6, D′–F′). In contrast, in Δp120-expressing neurons, bFGF addition was unable to stimulate any significant increase in the density of filopodia or SV puncta (Figure 6, G–I and G′–I′). These results, quantified in Figure 6, J and K, suggest that disruption of p120ctn/Rho signaling in spinal neurons blocked bFGF-induced filopodial assembly and SV clustering.

Effect of bFGF on p120ctn's tyrosine phosphorylation and cadherin association

Rho-family GTPases are potently regulated by p120ctn, which is not associated with cadherin, and the binding of p120ctn to cadherin is tightly controlled by the posttranslational modification of p120ctn (Reynolds, 2010). Previously we showed that treatment of muscle cells with agrin increased the tyrosine phosphorylation of p120ctn and decreased its association with cadherin (Madhavan *et al.*, 2006). Because expression of Rho-mutant p120ctn in neurons inhibited bFGF induction of filopodia and SV clusters (see earlier discussion), we tested whether signaling by bFGF can influence p120ctn in a cellular context. These experiments were carried out using NIH3T3-L1 fibroblasts because *Xenopus* neuron cultures provide insufficient

multiple 1-h Y27632-treatment experiments is shown in Figure 5, J and K; similar results were obtained from 6-h treatment experiments (unpublished data).

Taken together, the foregoing results suggest that p120ctn regulated filopodial assembly and SV clustering in *Xenopus* spinal neurons through Rho–ROCK signaling.

Function of p120ctn in bFGF-dependent axonal filopodial assembly and SV clustering

Previously we showed that polystyrene beads coated with bFGF induce SV clusters at sites where they contact cultured *Xenopus* spinal neurons (Dai and Peng, 1995), which suggests that bFGF is an inducer of presynaptic differentiation in neurons. More
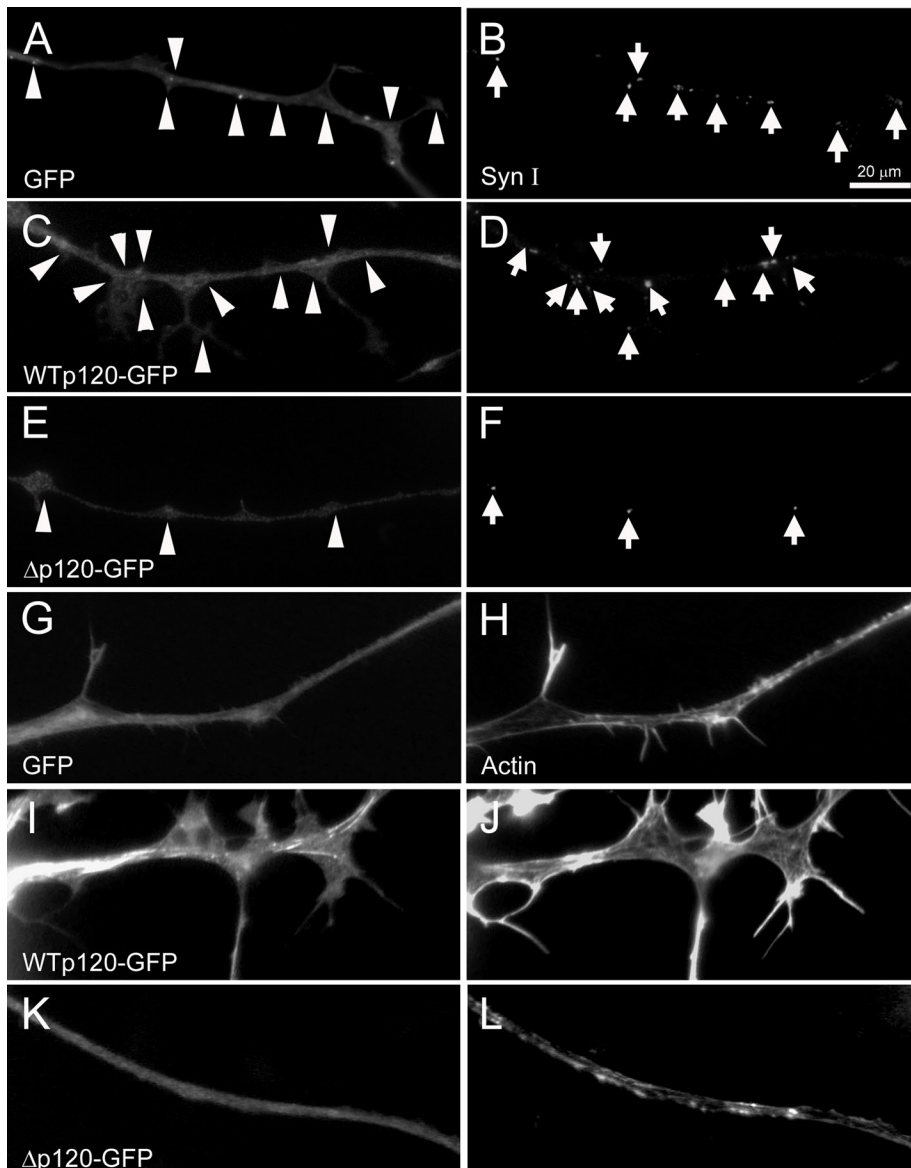
FIGURE 3: Induction of axonal filopodia and SV clusters by p120ctn and the association of F-actin with filopodia. In fixed cultures of control GFP-neurons, filopodia and SV clusters along axons could be detected by green fluorescence (A) and by anti–synapsin-I labeling (B), respectively. WTp120-neurons (C, D) grew more filopodia and showed more SV clusters than did control neurons, whereas Δp120-neurons (E, F) exhibited fewer filopodia and a reduced density of SV clusters. (G–L) Rhodamine-conjugated phalloidin was used to visualize F-actin enrichment in axons. In GFP axons (G, H) F-actin was enriched in filopodia, and in the WTp120-neurons (I, J), where more filopodia formed, F-actin labeling was also pronounced. (K, L) Axons expressing Δp120 had few filopodia and displayed correspondingly diminished F-actin labeling, except along the axonal shaft.

immunoblotting with phosphospecific anti–p120ctn antibodies to ask whether some of these sites were individually affected by bFGF. Our results showed that, relative to control, bFGF stimulation altered the phosphorylation profile of p120ctn: phosphorylation of p120ctn was significantly increased at Y280 but only slightly so at Y228 or Y291 (shown in Figure 7A with quantification). As a positive control, FGF receptor substrate 2α (FRS2α) was examined in parallel in these assays, and its tyrosine phosphorylation was found to be enhanced by bFGF (Figure 7B), as in many cell types (Eswarakumar et al., 2005). Of importance, by probing the immunoprecipitate of p120ctn we found that bFGF treatment led to ~30% decrease in the amount of cadherin associated with p120ctn (Figure 7C). Because p120ctn is known to exist in cadherin-associated and cadherin-free pools in cells (Reynolds, 2007), these results suggest that bFGF effected p120ctn's translocation from the former pool to the latter, possibly through the phosphorylation of Y280 and/or Y228/Y291 in p120ctn. Once in the cadherin-free pool, p120ctn could trigger cytoskeletal changes and generate motile processes by influencing the activity of Rho GTPases (Reynolds, 2007).

Neuronal p120ctn signaling and NMJ formation

In rodent nerve–muscle cocultures, myopodia facilitate tight interaction between nerve and muscle (Uhm et al., 2001). We previously showed that suppression of myopodial assembly in Xenopus muscle cells—by expressing the p120ctn-deletion mutant—inhibited NMJ development, which was observed as a marked reduction in AChR clustering at early nerve–muscle contacts (Madhavan et al., 2006). Recently we found that bFGF/FGFR1-dependent filopodial formation in spinal neurons also promotes nerve–muscle interaction and NMJ establishment (Li et al., 2011). Here we once again monitored nerve-induced AChR aggregation in muscle to test quantitatively whether synaptogenesis was affected when filopodial assembly in spinal neurons was blocked by disrupting p120ctn signaling. Spinal neurons were isolated from Xenopus embryos injected with mRNAs encoding GFP (Figure 8, A–C), WTp120 (Figure 8, D–F), or Δp120 (Figure 8, G–I), and these were seeded on muscle cells cultured 3 d earlier from embryos not injected with any mRNAs. This method ensures that any observed effects of the exogenous proteins are initiated solely on the presynaptic side. Cocultures were maintained for 22–24 h, and NMJ formation was examined by labeling with rhodamine-conjugated α-bungarotoxin (R-BTX). The results showed that, compared with cocultures using GFP- or WTp120-neurons, cultures prepared with Δp120-neurons had significantly less AChR clustering at innervation sites in muscle. Data were pooled from three

cellular material for biochemical assays; moreover, NIH3T3 cells were used in several past studies on both bFGF and p120ctn (Coleman et al., 2000; Noren et al., 2000).

NIH3T3-L1 cells were treated with or without bFGF, and total protein extracts were prepared. When p120ctn was immunoprecipitated from these extracts and initially examined, it was found to be heavily tyrosine phosphorylated, and this total phosphorylation (indicated by staining with anti–phosphotyrosine antibody mAb4G10) was not significantly increased after treatment of cells with bFGF (unpublished data). However, p120ctn is known to have many distinct tyrosine phosphorylation sites (Reynolds, 2007), and so we carried out
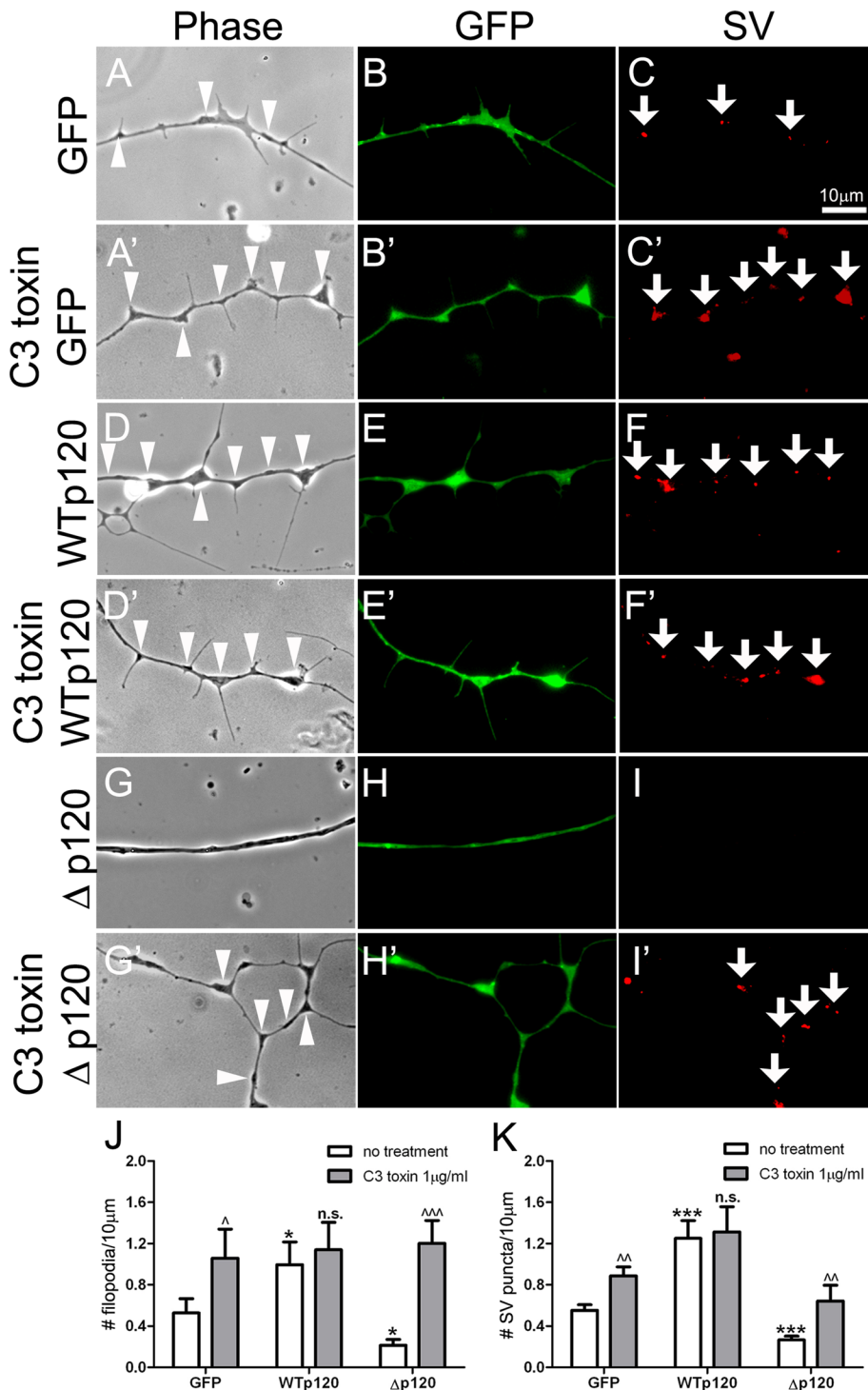
FIGURE 4: The effect of RhoA inhibitor C3 transferase on filopodial assembly and SV clustering. (A–C) Control neurons expressing GFP had filopodia and SV clusters along axons, and after treatment with C3 toxin (A'–C') they showed an increase in axonal filopodia and SV clustering. (D–F) WTp120 expression enhanced both filopodial assembly and SV clustering, and addition of C3 toxin to these neurons (D'–F') did not further elevate the effect. (G–I) Δp120 expression suppressed the formation of filopodia and SV clusters, and, significantly, this inhibitory effect of Δp120 was reversed in the presence of C3 toxin (G'–I'). These changes in the densities of filopodia and SV clusters are quantified in J and K. Mean and SEM are shown. *p < 0.05, ***p < 0.001, compared with control; ^p < 0.05, ^^p < 0.01, ^^^p < 0.001, compared with no treatment.

p120ctn was expressed in neurons, suggesting that normal p120ctn signaling in axons, which generates filopodia and SV clusters, facilitates neuromuscular synaptogenesis.

DISCUSSION

Actin polymerization and depolymerization control the formation of processes such as filopodia. An important intracellular regulator of actin cytoskeletal dynamics is p120ctn (Reynolds, 2007), which we showed promotes agrin-induced myopodial formation and NMJ establishment (Madhavan *et al.*, 2006). Others showed that p120ctn and δ-catenin enhance the assembly of filopodia and dendritic spines and synapses in CNS neurons (Arikkath and Reichardt, 2008). The results of this study suggest for the first time that p120ctn is involved in generating axonal filopodia in spinal neurons and that this is dependent on p120ctn signaling through Rho GTPases. The filopodial extension triggered by p120ctn was coupled with enhanced SV clustering in neurons, an indicator of presynaptic differentiation. Filopodia and SV clusters were also generated in neurons in response to bFGF, which is present on the muscle cell surface (Li *et al.*, 2011), but the bFGF effect was suppressed when p120ctn signaling in neurons was disrupted. If filopodial extension by nerve and muscle is considered as a "handshake" between the synaptic partners, this process could be seen as a prelude to the development of a lasting synapse. Of note, AChRs were clustered in muscle at sites contacted by neuronal filopodia, and blocking the formation of filopodia in neurons by perturbing p120ctn signaling reduced nerve-induced AChR clustering.

We chose to study p120ctn because it is expressed in neural tissues and because the filopodia that form in spinal neurons, naturally and in response to muscle and/or bFGF (Li *et al.*, 2011), resemble the filopodial processes that appear in many cell types after the overexpression of p120ctn. Whereas overexpression of wild-type p120ctn triggered filopodial assembly in spinal neurons, introduction of Rho-mutant p120ctn (Anastasiadis *et al.*, 2000) into neurons blocked both the normal formation of filopodia and bFGF's ability to induce them. That p120ctn promotes filopodial formation by suppressing Rho function was further suggested by experiments using the Rho inhibitor C3 toxin and an inhibitor of ROCK-1, a major effector of RhoA in cells. Treatment with either C3 toxin or Y27632 was able to rescue filopodial assembly in neurons expressing Rho-mutant p120ctn. Our Y27632 results are consistent with those of a previous study that identified ROCK as a negative regulator of

separate cocultures for each case, and the percentages of nerve–muscle contacts with AChR clusters were calculated. As shown in Figure 8J, NMJ formation was reduced by ~40% when Rho-mutant
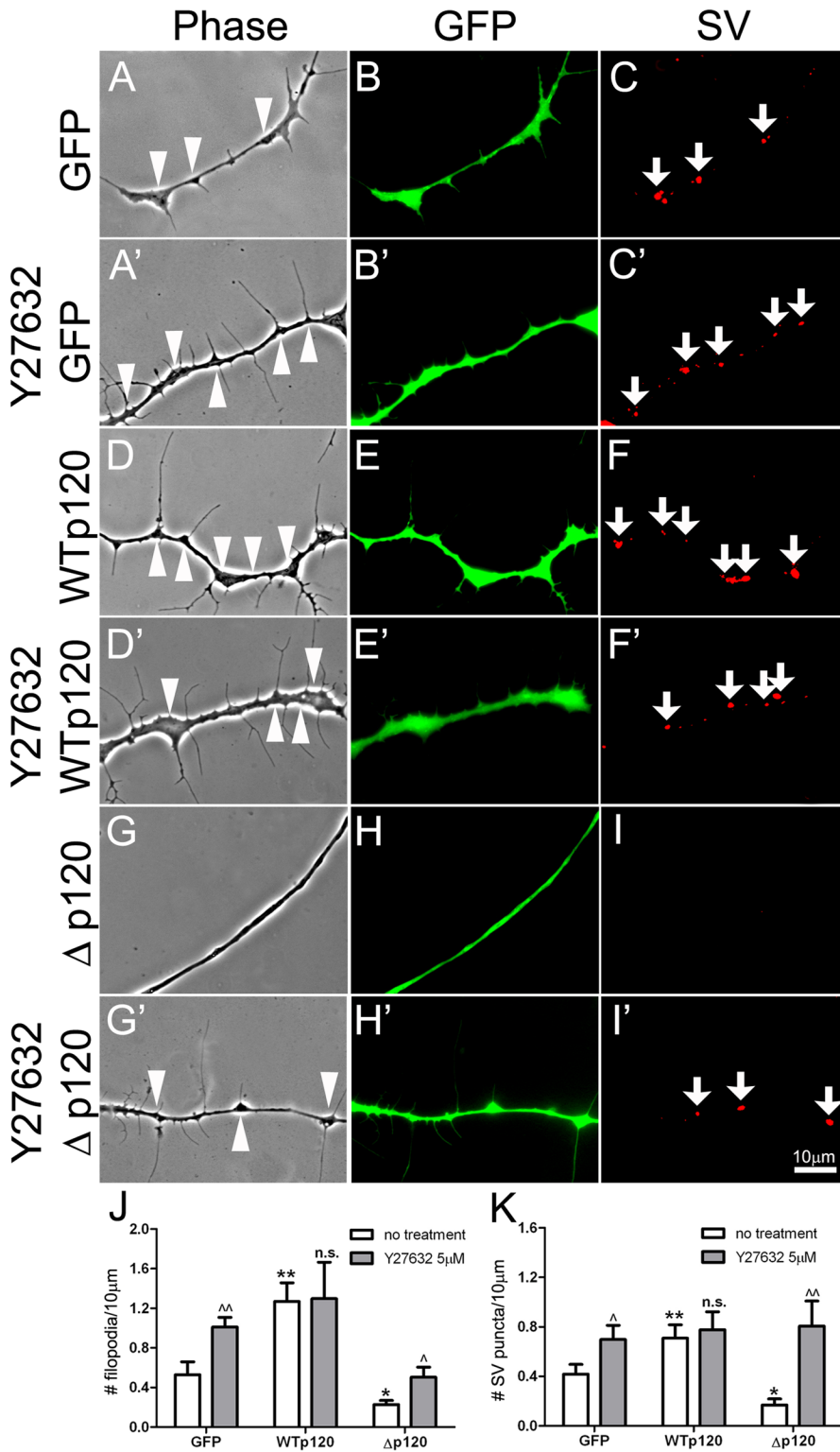
FIGURE 5: The effect of ROCK-1 inhibitor on filopodial assembly and SV clustering. The role of Rho GTPase signaling was further tested using Y27632, which inhibits the RhoA effector ROCK-1. (A–C) GFP-neurons developed filopodia and SV clusters along axons, and treatment with Y27632 (A'–C') increased axonal filopodia and SV clustering in these neurons. (D–F) WTp120 expression by itself increased filopodial formation and SV clustering in neurons, and this was not further elevated by treatment with the inhibitor (D'–F'). (G–I) Δp120 expression inhibited filopodial growth and SV clustering, and the suppressive effect of Δp120 was partially overcome in the presence of Y27632 (G'–I'). Both J and K quantify these changes in filopodial formation and SV clustering. Mean and SEM are shown. *p < 0.05, **p < 0.01, compared with control; ^p < 0.05, ^^p < 0.01, compared with no treatment.

F-actin–mediated protrusive activity of the axon (Loudon *et al.*, 2006). Although it remains to be determined what other GTPases and their effectors are targeted by p120ctn in spinal neurons, the changes seen in our experiments are in accord with the finding that deletion of p120ctn in central neurons leads to a decrease in Rac activity, an increase in Rho activity, and reduced dendritic spine formation (Elia *et al.*, 2006). It is worth noting here that under certain conditions p120ctn-mediated activation of Rac and Cdc42 may contribute to the ability of p120ctn to inhibit RhoA (Anastasiadis *et al.*, 2000).

The p120ctn protein, a major substrate of protein kinases and a core member of the cadherin complex (Reynolds, 2007), has myriad cellular functions: it influences cadherin surface expression, cell–cell interaction, cytoskeletal dynamics, Wnt signaling, and gene transcription (McCrea and Gu, 2010). The cytoskeletal effects of p120ctn depend to a large extent on p120ctn's ability to positively regulate Rac and Cdc42 GTPases and inhibit RhoA, which leads to increased cell motility and generates processes such as filopodia (Reynolds, 2007). The interaction of p120ctn with cadherin potently affects the modulation of GTPases by p120ctn, with the cadherin-free form of p120ctn being efficient at enhancing the activity of Rac/Cdc42 and suppressing that of Rho (Reynolds, 2007). Posttranslational modification of p120ctn intricately balances p120ctn's binding to and dissociation from cadherin (Reynolds, 2010), with reduced interaction of p120ctn with cadherin observed in muscle cells after agrin-stimulated tyrosine phosphorylation of p120ctn (Madhavan *et al.*, 2006). Here, in heterologous cells, signaling initiated by bFGF was able to significantly increase p120ctn's phosphorylation at Y280 (but only slightly at Y228 and Y291), and this was coupled with a reduction in the (biochemically detectable) interaction of p120ctn with cadherin. Although the effect of p120ctn's phosphorylation on cadherin binding is believed to be cadherin isoform dependent (Seidel *et al.*, 2004), our results raise the additional possibility that phosphorylation of only certain tyrosine residues in p120ctn, in response to factors such as bFGF, is important for controlling p120ctn–cadherin interaction. Whether this occurred in the neurons used in our study is not known because biochemical experiments could not be carried out on the spinal neurons cultured from *Xenopus* embryos and because the commercial phosphospecific anti-p120ctn antibodies failed to label fixed neurons (and muscle and other types of cells; R.M. and H.B.P., unpublished observations).

The view suggested by the results of this study and our previous work (Madhavan *et al.*, 2006) is that p120ctn facilitates NMJ assembly
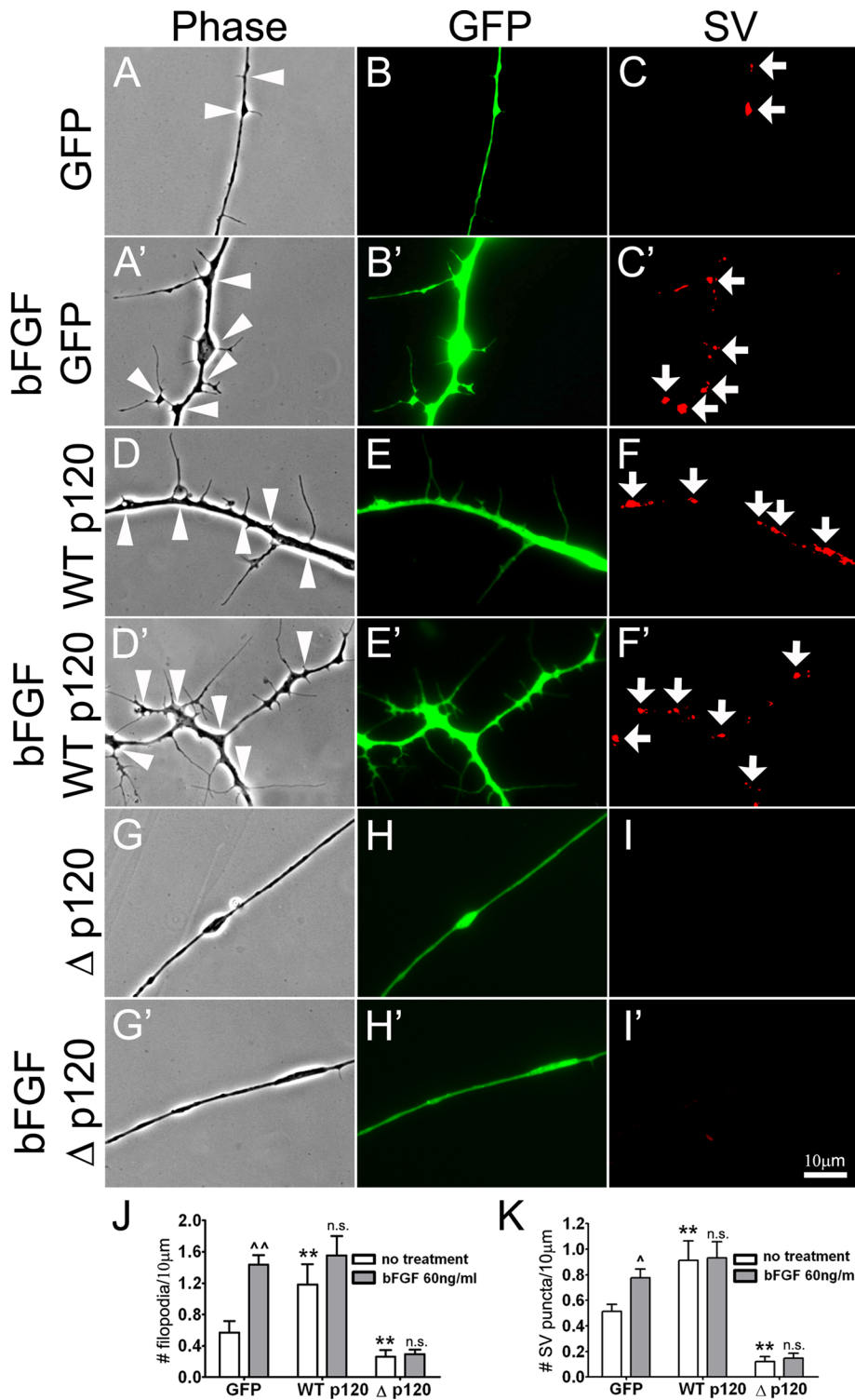
FIGURE 6: The effect of p120ctn on bFGF induction of filopodia and SV clusters in neurons. (A–C) Filopodial and SV cluster formation in control GFP-expressing neurons. (A'–C') Treatment with bFGF elevated the density of both filopodia and SV clusters. (D–F) Overexpression of WTp120 on its own increased these two axonal specializations, and treatment with bFGF (D'–F') slightly enhanced filopodial formation (see J for quantification). (G–I) Δp120 expression suppressed both specializations and also inhibited the effect of bFGF (G'–I') on filopodial and SV cluster induction. The densities of bFGF-induced filopodia (J) and SV clusters (K) were calculated from data pooled from three separate mRNA injections and culture preparations. Mean and SEM shown; t test, **$p < 0.01$, compared with control; ^$p < 0.05$, ^^$p < 0.01$, compared with no treatment.

by generating filopodial processes in nerve and muscle to promote synaptogenic interactions. In muscle we found that disruption of p120ctn signaling blocked the induction of myopodia by agrin and spinal neurons and inhibited synaptogenesis, but p120ctn did not directly influence AChR clustering itself (Madhavan *et al.*, 2006). Recently we showed that muscle and muscle-derived bFGF elicit filopodial growth in approaching axons (Li *et al.*, 2011), much like axons induce myopodia (Uhm *et al.*, 2001; Ritzenthaler and Chiba, 2003; Madhavan *et al.*, 2006). These neuronal filopodia, like their muscle counterparts, also appear to promote nerve–muscle interaction, since blocking their formation by inhibiting either bFGF/FGFR1 signaling (Li *et al.*, 2011) or p120ctn signaling (this study) hindered synaptogenesis. Another key finding of this study is that inhibition of p120ctn signaling reduced axonal SV clustering, both spontaneous and bFGF induced. This raises the possibility that bFGF and p120ctn, by mechanisms unknown but potentially involving Rho GTPases, together regulate presynaptic differentiation. Given that bFGF-coated beads can induce SV and mitochondrial clustering at bead–axon contacts (Dai and Peng, 1995; Lee and Peng, 2008), bFGF-activated FGFR1/p120ctn signaling might potentially facilitate the localized presynaptic induction and differentiation that occurs in a motor axon's growth cone after contact with muscle.

The present study suggests—to our knowledge for the first time—that p120ctn acts downstream from bFGF in filopodial formation in spinal neurons. Previous studies showed that p120ctn is a key mediator of the effects of diverse growth factors. In fibroblasts, for example, the remodeling of the actin cytoskeleton after the activation of platelet-derived growth factor receptor was blocked in the absence of p120ctn (Wildenberg *et al.*, 2006; Lee *et al.*, 2008). As a substrate for Src and other protein kinases, p120ctn also responds to the activation of the receptors for epidermal growth factor (EGF), colony-stimulating factor, and vascular endothelial growth factor and becomes phosphorylated on tyrosine, serine, and threonine residues (Downing and Reynolds, 1991; Esser *et al.*, 1998; Lee *et al.*, 2008). The relationship between EGF receptor and p120ctn is interesting in view of the present study because EGF stimulation triggered p120ctn phosphorylation at Y228; in our experiments Y280 of p120ctn showed the largest increase in phosphorylation in response to bFGF stimulation, and Y228 was phosphorylated to a lesser extent.
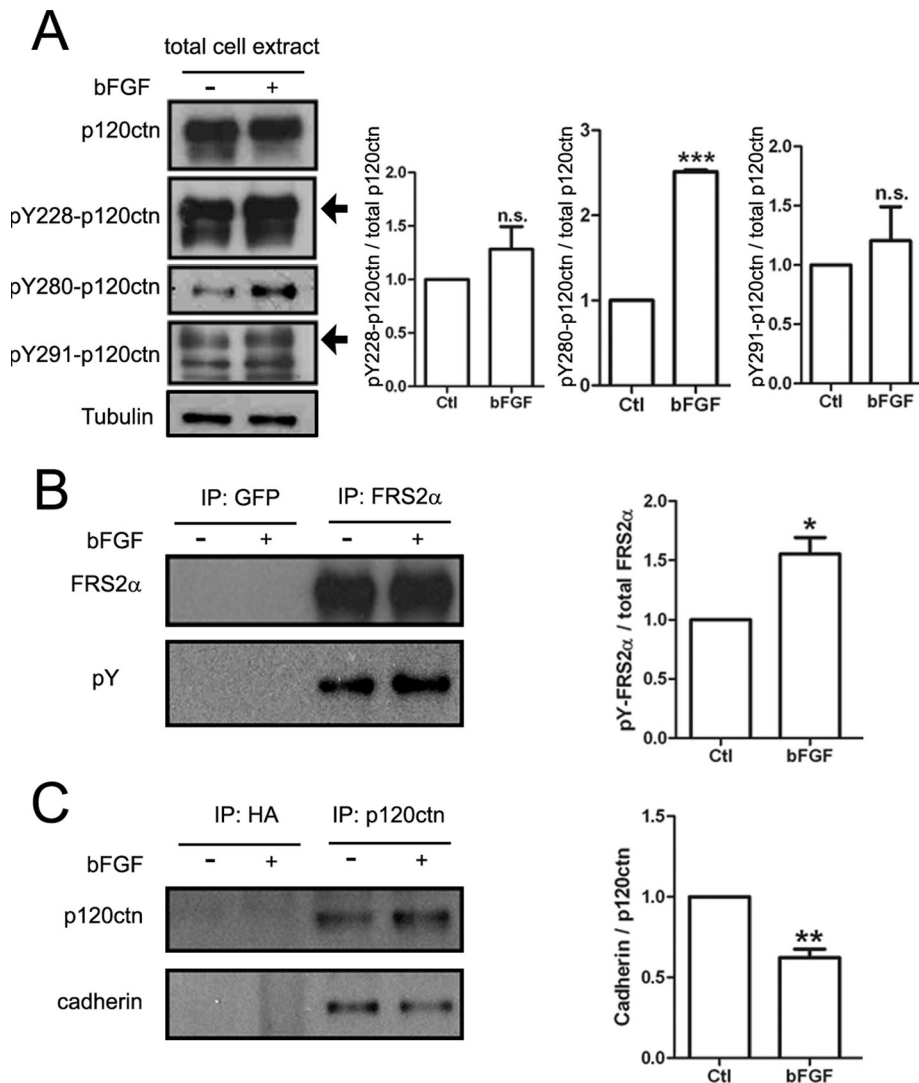
FIGURE 7: Influence of bFGF on p120ctn's tyrosine phosphorylation and cadherin association. NIH3T3-L1 fibroblasts were serum starved for 16–18 h and then stimulated for 30 min without (–) or with (+) bFGF (200 ng/ml) before preparing total protein extracts. (A) Extracts were immunoblotted with antibodies against p120ctn or p120ctn phosphorylated on three specific tyrosine residues (Y228, Y280, and Y291) and tubulin (loading control). Treatment with bFGF did not alter p120ctn levels in extracts, but it increased the phosphorylation of p120ctn at Y280 robustly and Y228 and Y291 slightly, as shown in the quantification on the right. (B) To confirm that bFGF stimulated the cells in these experiments, we also used a portion of the extracts for immunoprecipitating FRS2α, a downstream target of bFGF signaling. Staining with anti-FRS2α (top) and anti-phosphotyrosine mAb4G10 (pY; bottom) antibodies showed that bFGF stimulation significantly enhanced FRS2α's tyrosine phosphorylation (quantified on the right); a polyclonal GFP antibody used as a negative control did not capture FRS2α. (C) In parallel experiments when p120ctn was immunoprecipitated from extracts (top), under control conditions cadherin (bottom) coprecipitated with p120ctn, but the amount of cadherin associated with p120ctn was reduced by ~30% after bFGF treatment (quantified on the right); the control anti-hemagglutinin antibody captured neither p120ctn nor cadherin. Ratios of band densities presented in A–C were quantified from three replicates for each set. The ratios of samples from bFGF-treated cells were normalized relative to those from control to obtain the fold change produced by bFGF. Mean and SEM are shown. *p < 0.05, **p < 0.01, ***p < 0.001, compared with control.

Thus signals initiated by different growth factor receptors may target p120ctn at different but possibly also overlapping sites.

In fibroblasts p120ctn binds to N-cadherin, and the overexpression of p120ctn in these cells (which generates excess cadherin-free p120ctn) induces motile processes, including long, dendrite-like

structures (Reynolds et al., 1996). It is not known which isoforms of cadherin bind to p120ctn in spinal neurons, but the dissociation of p120ctn from one or more of these cadherins—after phosphorylation at sites like Y280 in response to stimulation by muscle-derived cues such as bFGF—might generate cadherin-free p120ctn in axons at levels sufficient for inducing the filopodia that initiate contacts with muscle. On the basis of this study and our previous work (Madhavan et al., 2006), we propose that p120ctn functions in mediating the effects of target-derived signals in both the presynaptic and postsynaptic sides of the NMJ during the earliest stages of synaptogenesis. Given that several FGFs and p120ctn have also been reported to promote the formation of CNS synapses (Arikkath and Reichardt, 2008; Lee et al., 2008; Terauchi et al., 2010), future manipulations of these molecules separately and together in central neurons could yield additional insights into the extent to which p120ctn influences the assembly and remodeling of synapses in the brain.

MATERIALS AND METHODS

Reagents

The following reagents were from commercial sources: bFGF (R&D Systems, Minneapolis, MN); FM4-64, rhodamine-conjugated phalloidin, and R-BTX (Molecular Probes, Eugene, OR); cell-permeant C3 transferase (Cytoskeleton, Denver, CO); Y27632 (Calbiochem, San Diego, CA); monoclonal antibodies against total p120ctn and phospho-Y228, -Y280, -Y291 p120ctn (BD/Transduction Laboratories, Lexington, KY); monoclonal p120ctn antibody, rabbit polyclonal FRS2 antibody, and protein A/G–agarose (Santa Cruz Biotechnology, Santa Cruz, CA); rabbit polyclonal pan-cadherin antibody (Zymed Laboratories, South San Francisco, CA); monoclonal anti-phosphotyrosine antibody mAb4G10 (Upstate Biotechnology, Lake Placid, NY); rabbit polyclonal synapsin-I antibody (Sigma-Aldrich, St. Louis, MO); horseradish peroxidase (HRP)–conjugated anti-mouse and anti-rabbit secondary antibodies (Jackson ImmunoResearch Laboratories, West Grove, PA); and Triton X-100 (Pierce, Rockford, IL).

Preparation of mRNAs encoding p120ctn proteins and embryo injection

The p120ctn proteins used here were generated with C-terminal GFP tags as previously described (Madhavan et al., 2006) by adding GFP-coding sequences to the cDNA of either wild-type mouse p120ctn (WTp120; Reynolds et al., 1992) or mutant p120ctn protein lacking a short internal sequence important for regulating Rho (Δp120ctn; Anastasiadis and Reynolds, 2001).

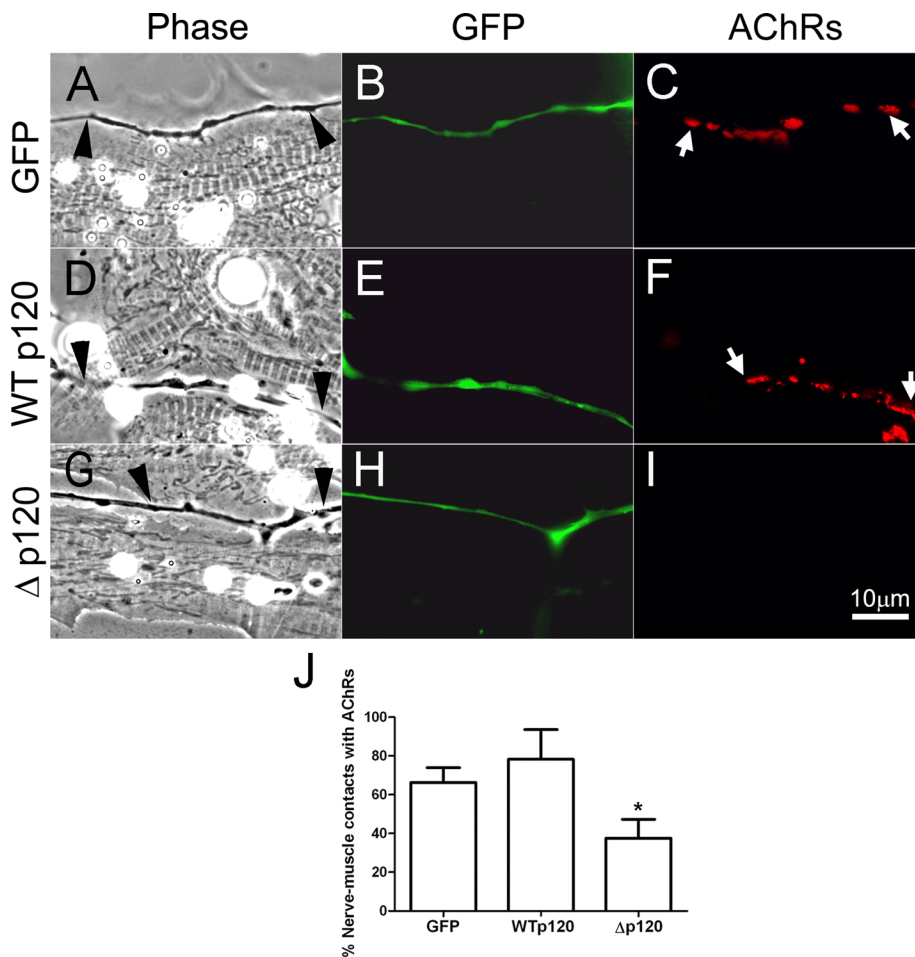|	Phase	GFP	AChRs
GFP	A	B	C
WT p120	D	E	F
Δ p120	G	H	I

10μm

J

FIGURE 8: The function of neuronal p120ctn in NMJ formation. Spinal neurons expressing GFP (A–C), WTp120 (D–F), or Rho-mutant Δp120 (G–I) were cocultured with 3-d-old muscle cells cultured from uninjected embryos, and NMJ formation along nerve–muscle contacts was examined after 1 d. The expression of exogenous proteins in spinal neurons was confirmed by GFP fluorescence, and labeling with R-BTX identified AChR clusters in muscle. Neurons expressing GFP (B) and WTp120ctn (E) effectively induced AChR clusters where they contacted muscle cells (C, F), with clusters present at 66.3 ± 7.7 and $78.3 \pm 15.3\%$ of contacts between muscle cells and GFP- and WTp120ctn-neurons, respectively (J). In contrast, Δp120ctn-expressing neurons (H) induced AChR clustering (I) at only $37.5 \pm 9.7\%$ of contacts with muscle cells (J). Arrowheads point to innervating axons, and arrows mark AChR clusters. Mean and SEM are shown. *$p < 0.05$, compared with control.

These cDNAs and one encoding GFP were linearized, and mRNAs were prepared from them using SP6 polymerase and the mMES-SAGE mMACHINE Kit (Ambion, Foster City, CA; Madhavan *et al.*, 2006). All mRNAs were injected into two-cell-stage *Xenopus* embryos using a Drummond Nanojet Oocyte Injector (Drummond Scientific Co., Broomall, PA). These injections introduced mRNAs into only a single cell of the two-cell embryos so that development could proceed, and embryos at stage 20–22 that exhibited GFP fluorescence were used for preparing neuron cultures.

Xenopus nerve and muscle primary cultures
Immunolabeling and ectopic expression experiments used primary cultures of *Xenopus* nerve and muscle cells prepared as described before (Peng *et al.*, 1991). In short, normal embryos or embryos injected with mRNAs were allowed to grow to stage 20–22 and then dissected; neural tubes and myotomes were separated and dissociated in a Ca^{2+}/Mg^{2+}-free solution, and the dissociated cells were plated on glass coverslips coated with entactin–collagen IV–laminin

(E-C-L) substrate (Upstate Biotechnology, Waltham, MA). Nerve–muscle cocultures were prepared by seeding neurons from normal or mRNA-injected embryos on 3-d-old muscle cultures prepared from uninjected embryos.

Growth factor/inhibitor treatment, labeling, and microscopy
Cultured spinal neurons were incubated with bFGF (60 ng/ml; 6 h), Y27632 (5 μM; 1 or 6 h), or C3 toxin (1 μg/ml; 1 h) before examination. To visualize SV puncta in live neuron cultures, we stained cells with 15 μM FM4-64 for 2 min in a high-potassium solution (30 mM NaCl, 51 mM KCl, 2 mM $CaCl_2$, and 5 mM 4-(2-hydroxyethyl)-1-piperazineethanesulfonic acid [HEPES], pH 7.4) and then washed them thrice with a modified Ringer solution (80 mM NaCl, 1 mM KCl, 2 mM $CaCl_2$, and 5 mM HEPES, pH 7.4) before examination by fluorescence microscopy. For time-lapse recording, images of neurons expressing GFP, WTp120-GFP, or Δp120ctn-GFP were taken at 1-min intervals over 10 min to monitor filopodial dynamics; rates of new filopodial formation in different neurons were quantified from these image sets and normalized relative to GFP-neurons.

In some experiments neurons were fixed with paraformaldehyde and then stained with primary and fluorescent secondary antibodies or with rhodamine-conjugated phalloidin. To study synapse formation, we labeled nerve–muscle cocultures with 3 nM R-BTX. In live cultures nerve–muscle contacts were identified in phase-contrast and AChR clusters by fluorescence microscopy. NMJ formation was quantified by calculating the percentages of nerve–muscle contacts with AChR clusters. Cultures were examined using a 63× oil-immersion lens and a custom-made "live chamber" that sealed

in cells and medium. Images were captured using a Zeiss Axiovert 200M microscope attached to a Zeiss AxioCamMR camera (Carl Zeiss, Jena, Germany). The camera was controlled by AxioVision Pel 4.5 software, which was also used for image processing. All data are presented as mean ± SEM values, and differences between groups were assessed using nonpaired Student's *t* tests carried out by Prism statistical software (GraphPad, La Jolla, CA).

Immunoprecipitation and immunoblotting
NIH3T3-L1 cells were cultured in DMEM containing 10% fetal bovine serum (FBS) and 1% penicillin–streptomycin. Cells were serum starved in DMEM containing 0.1% FBS and 1% penicillin–streptomycin for 16–18 h before stimulation with bFGF (200 ng/ml; 30 min); pervanadate (100 μM) was included to suppress tyrosine phosphatase activity and allow the detection of phosphorylated proteins. Fresh pervanadate was made just before use by mixing 10 mM Na orthovanadate with 1.7% H_2O_2 (50:1 ratio, 10 min, room temperature); this was diluted into culture medium (Madhavan *et al.*, 2006).

For immunoprecipitation and immunoblotting assays, cells were lysed (3 min at 0°C) in ice-cold IP buffer (25 mM HEPES, pH 7.4, 150 mM NaCl, 1 mM EDTA, 1% Triton X-100) containing the protease inhibitor phenylmethylsulfonyl fluoride (1 mM) and pervanadate (1 mM). Lysates were sonicated and clarified by centrifugation for 30 min, and a part of the extract was mixed immediately with 2× SDS-electrophoresis sample buffer (for blotting total proteins). For immunoprecipitation, 1–2 µg of antibodies was added to 0.4- to 0.6-ml extracts together with 15 µl of protein A/G–agarose slurry, and the mixtures were incubated for 3 h at 4°C with end-over-end rotation. Beads were spun down, washed thrice with 700 µl of IP buffer, and then resuspended in 30–50 µl of SDS-sample buffer. Eluted proteins were separated by 8% SDS–PAGE and transferred to polyvinylidene fluoride membranes, which were blocked (with 4% BSA) before probing with primary and HRP-conjugated secondary antibodies for detecting proteins of interest by enhanced chemiluminescence (West Pico; Pierce).

To quantify changes in protein phosphorylation and coimmunoprecipitation, we determined the density of each band in scanned immunoblot images using ImageJ software (National Institutes of Health, Bethesda, MD). Because the overall gray density levels of blots varied from experiment to experiment, the ratio of test (bFGF treatment) to control band density was calculated for each case separately (after correcting for protein loading) to estimate the extent of change in each experiment. From these ratios the mean and SE of the mean for test samples were calculated and plotted. Statistical analyses using Student's *t* test were carried out for each study.

REFERENCES
Aktories K, Just I (2005). Clostridial Rho-inhibiting protein toxins. Curr Top Microbiol Immunol 291, 113–145.

Anastasiadis PZ, Moon SY, Thoreson MA, Mariner DJ, Crawford HC, Zheng Y, Reynolds AB (2000). Inhibition of RhoA by p120 catenin. Nat Cell Biol 2, 637–644.

Anastasiadis PZ, Reynolds AB (2001). Regulation of Rho GTPases by p120-catenin. Curr Opin Cell Biol 13, 604–610.

Arikkath J, Reichardt LF (2008). Cadherins and catenins at synapses: roles in synaptogenesis and synaptic plasticity. Trends Neurosci 31, 487–494.

Banks GB, Fuhrer C, Adams ME, Froehner SC (2003). The postsynaptic submembrane machinery at the neuromuscular junction: requirement for rapsyn and the utrophin/dystrophin-associated complex. J Neurocytol 32, 709–726.

Brigidi GS, Bamji SX (2011). Cadherin-catenin adhesion complexes at the synapse. Curr Opin Neurobiol 21, 208–214.

Buchanan J, Sun YA, Poo MM (1989). Studies of nerve-muscle interactions in *Xenopus* cell culture: fine structure of early functional contacts. J Neurosci 9, 1540–1554.

Ciesiolka M, Delvaeye M, Van Imschoot G, Verschuere V, McCrea P, van Roy F, Vleminckx K (2004). p120 catenin is required for morphogenetic movements involved in the formation of the eyes and the craniofacial skeleton in *Xenopus*. J Cell Sci 117, 4325–4339.

Coleman AB, Momand J, Kane SE (2000). Basic fibroblast growth factor sensitizes NIH 3T3 cells to apoptosis induced by cisplatin. Mol Pharmacol 57, 324–333.

Dai Z, Peng HB (1995). Presynaptic differentiation induced in cultured neurons by local application of basic fibroblast growth factor. J Neurosci 15, 5466–5475.

Dai Z, Peng HB (1996). Dynamics of synaptic vesicles in cultured spinal cord neurons in relationship to synaptogenesis. Mol Cell Neurosci 7, 443–452.

Dent EW, Tang F, Kalil K (2003). Axon guidance by growth cones and branches: common cytoskeletal and signaling mechanisms. Neuroscientist 9, 343–353.

Downing JR, Reynolds AB (1991). PDGF, CSF-1, and EGF induce tyrosine phosphorylation of p120, a pp60src transformation-associated substrate. Oncogene 6, 607–613.

Elia LP, Yamamoto M, Zang K, Reichardt LF (2006). p120 catenin regulates dendritic spine and synapse development through Rho-family GTPases and cadherins. Neuron 51, 43–56.

Esser S, Lampugnani MG, Corada M, Dejana E, Risau W (1998). Vascular endothelial growth factor induces VE-cadherin tyrosine phosphorylation in endothelial cells. J Cell Sci 111, 1853–1865.

Eswarakumar VP, Lax I, Schlessinger J (2005). Cellular signaling by fibroblast growth factor receptors. Cytokine Growth Factor Rev 16, 139–149.

Fang X, Ji H, Kim SW, Park JI, Vaught TG, Anastasiadis PZ, Ciesiolka M, McCrea PD (2004). Vertebrate development requires ARVCF and p120 catenins and their interplay with RhoA and Rac. J Cell Biol 165, 87–98.

Fertuck HC, Salpeter MM (1976). Quantitation of junctional and extrajunctional acetylcholine receptors by electron microscope autoradiography after 125I-alpha-bungarotoxin binding at mouse neuromuscular junctions. J Cell Biol 69, 144–158.

Fitzsimonds RM, Poo MM (1998). Retrograde signaling in the development and modification of synapses. Physiol Rev 78, 143–170.

Fox MA et al. (2007). Distinct target-derived signals organize formation, maturation, and maintenance of motor nerve terminals. Cell 129, 179–193.

Fox MA, Umemori H (2006). Seeking long-term relationship: axon and target communicate to organize synaptic differentiation. J Neurochem 97, 1215–1231.

Gallo G, Letourneau PC (2004). Regulation of growth cone actin filaments by guidance cues. J Neurobiol 58, 92–102.

Glass DJ et al. (1996). Agrin acts via a MuSK receptor complex. Cell 85, 513–523.

Glass DJ, Yancopoulos GD (1997). Sequential roles of agrin, MuSK and rapsyn during neuromuscular junction formation. Curr Opin Neurobiol 7, 379–384.

Harris KM, Kater SB (1994). Dendritic spines: cellular specializations imparting both stability and flexibility to synaptic function. Annu Rev Neurosci 17, 341–371.

Hotulainen P, Llano O, Smirnov S, Tanhuanpaa K, Faix J, Rivera C, Lappalainen P (2009). Defining mechanisms of actin polymerization and depolymerization during dendritic spine morphogenesis. J Cell Biol 185, 323–339.

Hughes BW, Kusner LL, Kaminski HJ (2006). Molecular architecture of the neuromuscular junction. Muscle Nerve 33, 445–461.

Ishizaki T, Uehata M, Tamechika I, Keel J, Nonomura K, Maekawa M, Narumiya S (2000). Pharmacological properties of Y-27632, a specific inhibitor of rho-associated kinases. Mol Pharmacol 57, 976–983.

Johnson-Venkatesh EM, Umemori H (2010). Secreted factors as synaptic organizers. Eur J Neurosci 32, 181–190.

Lee CW, Peng HB (2006). Mitochondrial clustering at the vertebrate neuromuscular junction during presynaptic differentiation. J Neurobiol 66, 522–536.

Lee CW, Peng HB (2008). The function of mitochondria in presynaptic development at the neuromuscular junction. Mol Biol Cell 19, 150–158.

Lee SH et al. (2008). Synapses are regulated by the cytoplasmic tyrosine kinase Fer in a pathway mediated by p120catenin, Fer, SHP-2, and beta-catenin. J Cell Biol 183, 893–908.

Li PP, Chen C, Lee CW, Madhavan R, Peng HB (2011). Axonal filopodial asymmetry induced by synaptic target. Mol Biol Cell 22, 2480–2490.

Lin CH, Forscher P (1993). Cytoskeletal remodeling during growth cone-target interactions. J Cell Biol 121, 1369–1383.

Loudon RP, Silver LD, Yee HF Jr, Gallo G (2006). RhoA-kinase and myosin II are required for the maintenance of growth cone polarity and guidance by nerve growth factor. J Neurobiol 66, 847–867.

Mackay DJ, Nobes CD, Hall A (1995). The Rho's progress: a potential role during neuritogenesis for the Rho family of GTPases. Trends Neurosci 18, 496–501.

Madhavan R, Peng HB (2005). Molecular regulation of postsynaptic differentiation at the neuromuscular junction. IUBMB Life 57, 719–730.

Madhavan R, Zhao XT, Reynolds AB, Peng HB (2006). Involvement of p120 catenin in myopodial assembly and nerve-muscle synapse formation. J Neurobiol 66, 1511–1527.

McCrea PD, Gu D (2010). The catenin family at a glance. J Cell Sci 123, 637–642.

Nakajima Y, Kidokoro Y, Klier FG (1980). The development of functional neuromuscular junctions in vitro: an ultrastructural and physiological study. Dev Biol 77, 52–72.

Nobes CD, Hall A (1995). Rho, rac, and cdc42 GTPases regulate the assembly of multimolecular focal complexes associated with actin stress fibers, lamellipodia, and filopodia. Cell 81, 53–62.

Noren NK, Liu BP, Burridge K, Kreft B (2000). p120 catenin regulates the actin cytoskeleton via Rho family GTPases. J Cell Biol 150, 567–580.

Olivo C, Vanni C, Mancini P, Silengo L, Torrisi MR, Tarone G, Defilippi P, Eva A (2000). Distinct involvement of cdc42 and RhoA GTPases in actin organization and cell shape in untransformed and Dbl oncogene transformed NIH3T3 cells. Oncogene 19, 1428–1436.

Paulson AF, Fang X, Ji H, Reynolds AB, McCrea PD (1999). Misexpression of the catenin p120(ctn)1A perturbs *Xenopus* gastrulation but does not elicit Wnt-directed axis specification. Dev Biol 207, 350–363.

Peng HB, Baker LP, Chen Q (1991). Tissue culture of *Xenopus* neurons and muscle cells as a model for studying synaptic induction. Methods Cell Biol 36, 511–526.

Reynolds AB (2007). p120-catenin: past and present. Biochim Biophys Acta 1773, 2–7.

Reynolds AB (2010). Exposing p120 catenin's most intimate affair. Cell 141, 20–22.

Reynolds AB, Daniel JM, Mo YY, Wu J, Zhang Z (1996). The novel catenin p120cas binds classical cadherins and induces an unusual morphological phenotype in NIH3T3 fibroblasts. Exp Cell Res 225, 328–337.

Reynolds AB, Herbert L, Cleveland JL, Berg ST, Gaut JR (1992). p120, a novel substrate of protein tyrosine kinase receptors and of p60v-src, is related to cadherin-binding factors beta-catenin, plakoglobin and armadillo. Oncogene 7, 2439–2445.

Reynolds AB, Roesel DJ, Kanner SB, Parsons JT (1989). Transformation-specific tyrosine phosphorylation of a novel cellular protein in chicken cells expressing oncogenic variants of the avian cellular src gene. Mol Cell Biol 9, 629–638.

Ritzenthaler S, Chiba A (2003). Myopodia (postsynaptic filopodia) participate in synaptic target recognition. J Neurobiol 55, 31–40.

Seidel B, Braeg S, Adler G, Wedlich D, Menke A (2004). E- and N-cadherin differ with respect to their associated p120ctn isoforms and their ability to suppress invasive growth in pancreatic cancer cells. Oncogene 23, 5532–5542.

Siksou L, Triller A, Marty S (2011). Ultrastructural organization of presynaptic terminals. Curr Opin Neurobiol 21, 261–268.

Terauchi A, Johnson-Venkatesh EM, Toth AB, Javed D, Sutton MA, Umemori H (2010). Distinct FGFs promote differentiation of excitatory and inhibitory synapses. Nature 465, 783–787.

Uhm CS, Neuhuber B, Lowe B, Crocker V, Daniels MP (2001). Synapse-forming axons and recombinant agrin induce microprocess formation on myotubes. J Neurosci 21, 9678–9689.

Weldon PR, Cohen MW (1979). Development of synaptic ultrastructure at neuromuscular contacts in an amphibian cell culture system. J Neurocytol 8, 239–259.

Wildenberg GA, Dohn MR, Carnahan RH, Davis MA, Lobdell NA, Settleman J, Reynolds AB (2006). p120-catenin and p190RhoGAP regulate cell-cell adhesion by coordinating antagonism between Rac and Rho. Cell 127, 1027–1039.